

# Supporting Information

## Electron transfer coupled spin transition in cyano-bridged mixed-valence $\{\text{Fe}^{\text{III}}_2\text{Fe}^{\text{II}}_2\}$ molecular squares

Shuwen Jia, Mengjia Shang, Sai Jin, Xinrui Zhu, Yuanyuan Cai and Dongfeng Li\*

Key Laboratory of Pesticide and Chemical Biology of Ministry of Education, College of Chemistry,  
Central China Normal University, 430079 Wuhan, P. R. China.  
E-mail: dfli@mail.ccnu.edu.cn.

## CONTENTS

<b>Figure S1.</b> $^1\text{H}$ NMR (400 MHz) of bnbpen, in $\text{CDCl}_3$ .....	3
<b>Figure S2.</b> $^{13}\text{C}$ NMR (100 MHz) of bnbpen, in $\text{CDCl}_3$ .....	3
<b>Figure S3.</b> ESI-MS spectrum for <b>1</b> ·8CH <sub>3</sub> OH in MeCN.....	4
<b>Figure S4.</b> Thermogravimetric analysis of <b>1</b> ·8CH <sub>3</sub> OH (a) and <b>1</b> (b). ....	4
<b>Figure S5.</b> The molecular structure of <b>1</b> .....	5
<b>Table S1.</b> Crystal data and structure refinement for <b>1</b> ·8CH <sub>3</sub> OH.....	6
<b>Table S2.</b> Selected bond lengths ( $\text{\AA}$ ) of <b>1</b> ·8CH <sub>3</sub> OH at different temperatures. ....	7
<b>Table S3.</b> Selected bond angles ( $^\circ$ ) of <b>1</b> ·8CH <sub>3</sub> OH at different temperatures. ....	8
<b>Table S4.</b> Crystal data and structure refinement for <b>1</b> .....	9
<b>Table S5.</b> Selected bond lengths ( $\text{\AA}$ ) of <b>1</b> at different temperatures.....	10
<b>Table S6.</b> Selected bond angles ( $^\circ$ ) of <b>1</b> at different temperatures. ....	11
<b>Table S7.</b> Structural parameters for <b>1</b> ·8CH <sub>3</sub> OH and <b>1</b> at high and low temperature. 12	12
<b>Figure S7.</b> IR spectra for <b>1</b> ·8CH <sub>3</sub> OH and <b>1</b> at room temperature. ....	12
<b>Figure S8.</b> Variable temperature solid state FT–IR spectra for <b>1</b> ·8CH <sub>3</sub> OH .....	13
<b>Figure S9.</b> Variable temperature solid state FT–IR spectra for <b>1</b> .....	13
<b>Figure S10.</b> Variable–temperature solid–state UV–vis spectra .....	13
<b>Figure S11.</b> Plots of $d\chi/T/dT$ vs. temperature for <b>1</b> ·8CH <sub>3</sub> OH and <b>1</b> . ....	14
<b>Figure S12.</b> Plots of $\chi_M T$ vs. temperature for <b>1</b> ·8CH <sub>3</sub> OH and <b>1</b> .....	14
<b>Figure S13.</b> $^{57}\text{Fe}$ Mössbauer spectra of <b>1</b> ·8CH <sub>3</sub> OH.....	14
<b>Table S8.</b> Mössbauer spectrum data of <b>1</b> ·8CH <sub>3</sub> OH and <b>1</b> .....	15
<b>Figure S14.</b> Packing diagrams of <b>1</b> ·8CH <sub>3</sub> OH .....	16
<b>Figure S15.</b> Packing diagrams of <b>1</b> .....	17
<b>Figure S16.</b> Hirshfeld surface of <b>1</b> ·8CH <sub>3</sub> OH .....	18
<b>Figure S17.</b> Hirshfeld surface of <b>1</b> .....	18

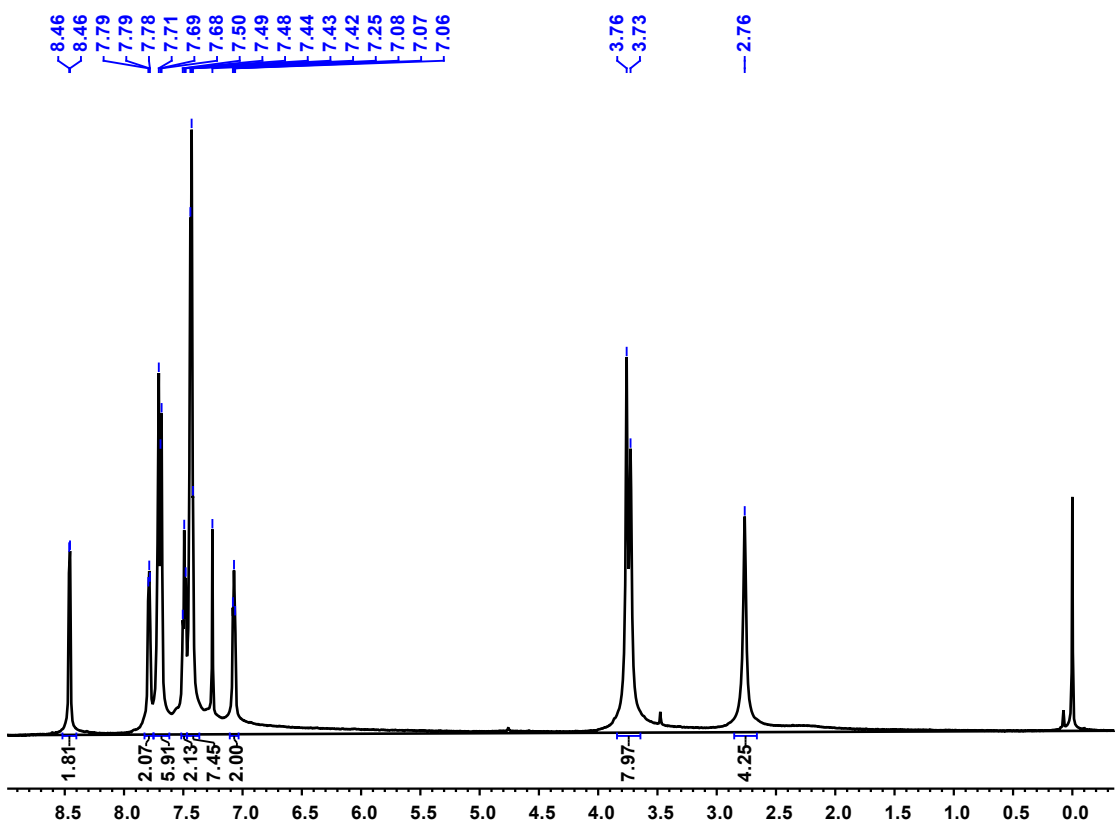


**Figure S1.**  $^1\text{H}$  NMR (400 MHz) of bnbpen, in  $\text{CDCl}_3$ .

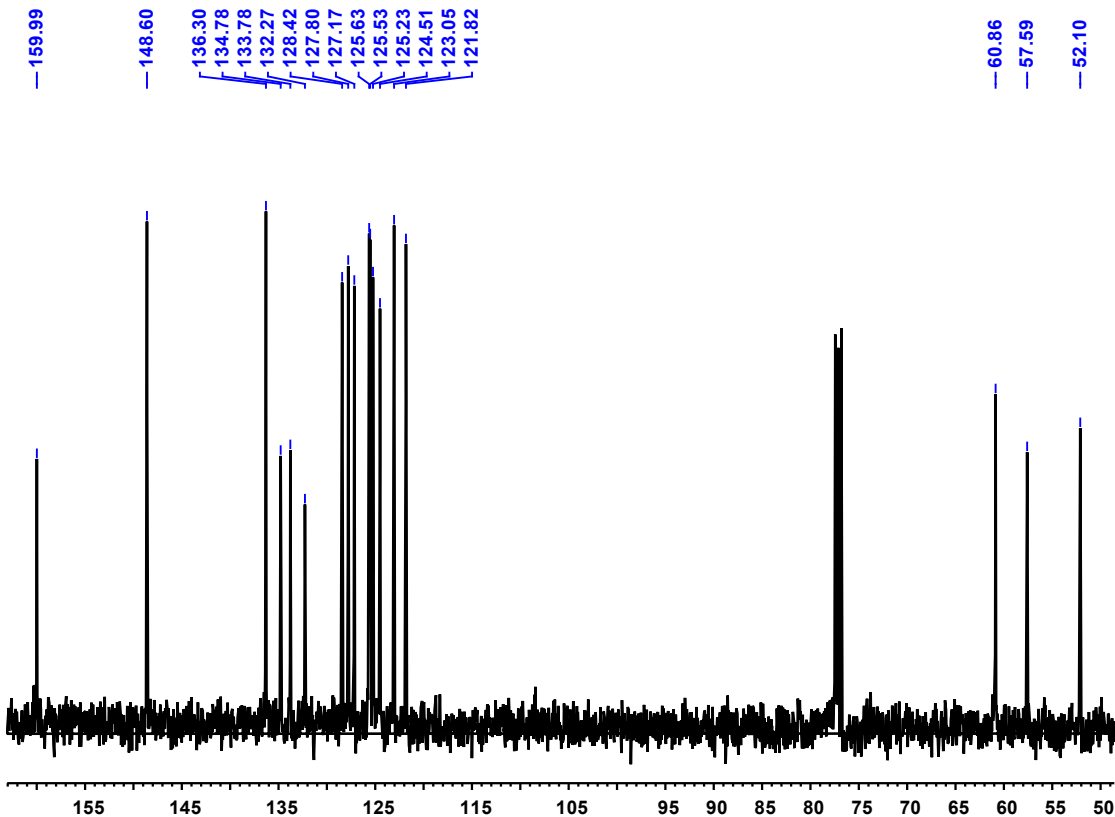


**Figure S2.**  $^{13}\text{C}$  NMR (100 MHz) of bnbpen, in  $\text{CDCl}_3$ .

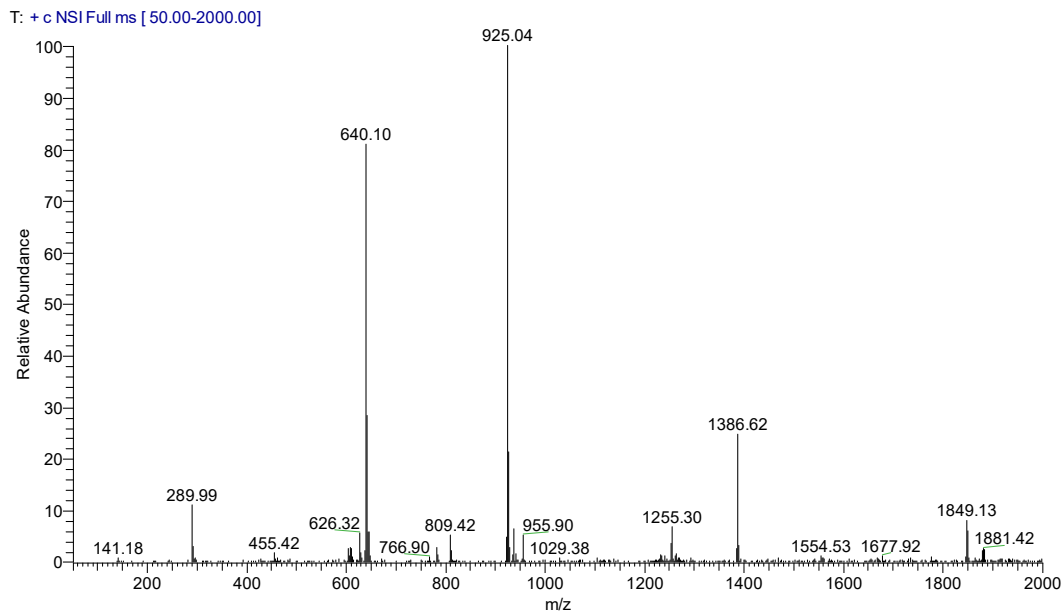


**Figure S3.** ESI-MS spectrum for **1**·8CH<sub>3</sub>OH in MeCN.

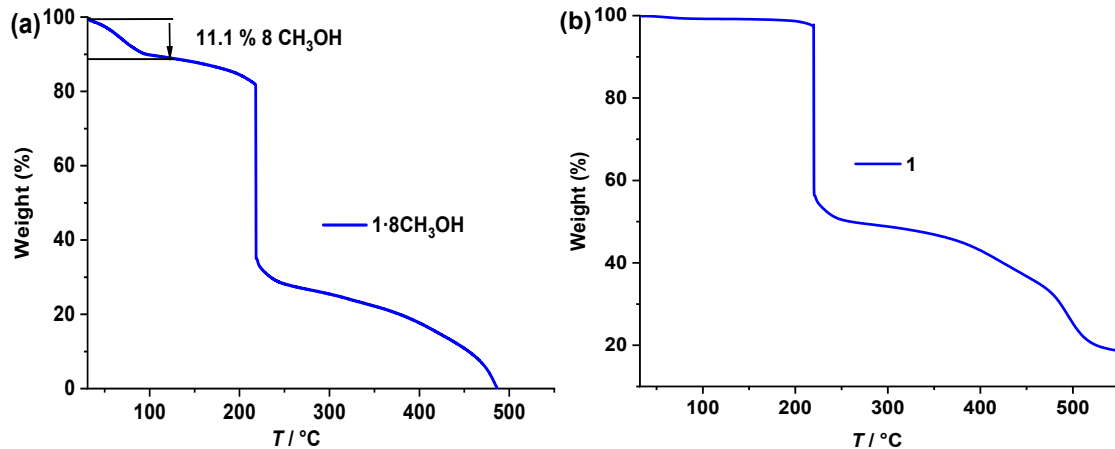


**Figure S4.** Thermogravimetric analysis of **1**·8CH<sub>3</sub>OH (a) and **1** (b).

For **1**·8CH<sub>3</sub>OH, the first weight loss until 122 °C was due to the loss of weight CH<sub>3</sub>OH molecules (obsd 11.1%, cacl 11.1%). The decomposition of the organic links in the solvent-free compound occurs at 218 °C. For **1**, no solvent molecules are present in the structure. The decomposition of the organic links in the solvent-free compound occurs at 220 °C.

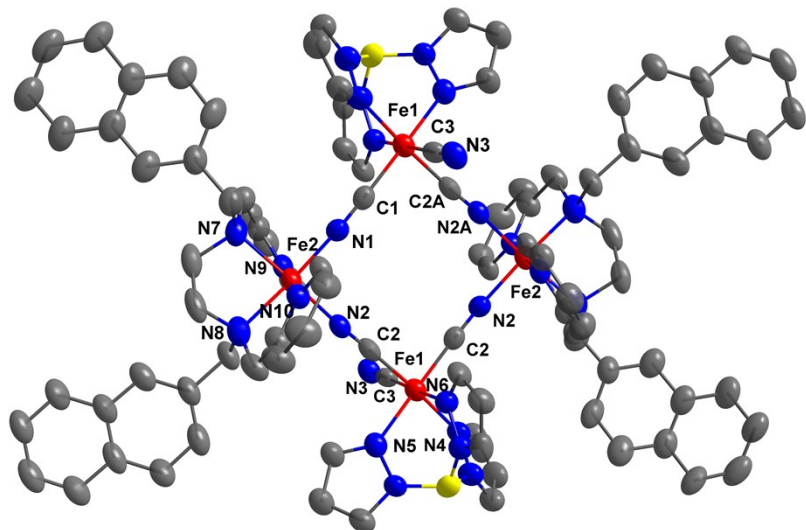


**Figure S5.** The molecular structure of **1** at 298 K (symmetry code A:  $-x+2$ ,  $-y+1$ ,  $-z+2$ ), anions, and hydrogen atoms are omitted for clarity. Lattice solvent molecules, anions, and hydrogen atoms are omitted for clarity. C gray, Fe red, N blue, B yellow.

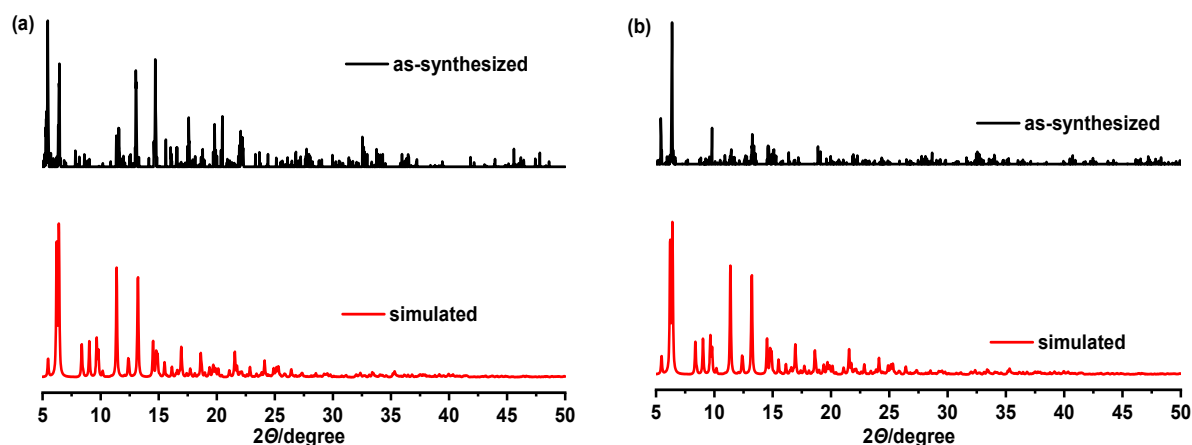


**Figure S6.** X-ray powder diffraction pattern of **1**· $8\text{CH}_3\text{OH}$  (a) and f **1** (b), and the simulated pattern from single crystal data.

**Table S1.** Crystal data and structure refinement for **1·8CH<sub>3</sub>OH**.

Compound	1·8CH <sub>3</sub> OH		
CCDC	2183791	2215522	2215521
T(K)	298	165	100
Formula	C <sub>104</sub> H <sub>120</sub> B <sub>2</sub> Fe <sub>4</sub> N <sub>26</sub> Cl <sub>2</sub> O <sub>16</sub>		
Formula weight	2306.2		
Crystal system	Triclinic		
Space group	P $\bar{1}$		
Z	1		
a / Å	11.103(7)	11.006(9)	10.964(2)
b / Å	16.132(3)	15.852(4)	15.816(9)
c / Å	17.708(3)	17.6035(16)	17.507(2)
$\alpha$ / °	111.734(7)	111.570(3)	111.488(5)
$\beta$ / °	93.802(7)	93.521(4)	93.295(5)
$\gamma$ / °	106.978(6)	106.655(3)	106.620(4)
V / Å <sup>3</sup>	2763.0(8)	2687.9(4)	2661.6(5)
$d_{calc}$ (mg/m <sup>3</sup> )	1.232	1.266	1.279
$\mu$ / mm <sup>-1</sup>	3.48	3.58	3.61
F(000)	1058	1058	1058
Collected reflections	48878	39555	45600
Unique reflections	9293	8821	8737
$R_{int}$	0.078	0.069	0.059
Goodness-of-fit on $F^2$	1.06	1.06	1.06
$R_1$ [ $ I  > 2\sigma (I)$ ]	0.062	0.054	0.038
wR <sub>2</sub> [ $ I  > 2\sigma (I)$ ]	0.185	0.156	0.107

$$R_1 = \sum (|F_o| - |F_c|) / \sum |F_o|; wR_2 = [\sum w (|F_o| - |F_c|)^2 / \sum w F_o^2]^{1/2}.$$

**Table S2.** Selected bond lengths (Å) of **1**·8CH<sub>3</sub>OH at different temperatures.

	<b>1</b> ·8CH <sub>3</sub> OH <sup>298</sup> K	<b>1</b> ·8CH <sub>3</sub> OH <sup>165</sup> K	<b>1</b> ·8CH <sub>3</sub> OH <sup>100</sup> K
Fe1-C1	1.933(3)	1.876(3)	1.865(2)
Fe1-C2	1.912(4)	1.867(3)	1.862(2)
Fe1-C3	1.936(4)	1.930(4)	1.922(3)
Fe1-N4	1.997(3)	2.002(3)	2.003(2)
Fe1-N5	1.997(3)	2.007(3)	2.011(2)
Fe1-N6	1.984(3)	1.994(3)	1.995(2)
Fe2-N1	2.121(3)	2.022(3)	1.993(2)
Fe2-N2	2.121(3)	2.024(3)	1.994(2)
Fe2-N7	2.282(3)	2.240(3)	2.225(2)
Fe2-N8	2.286(3)	2.246(3)	2.232(2)
Fe2-N9	2.193(3)	2.150(3)	2.132(2)
Fe2-N10	2.201(3)	2.164(3)	2.144(2)
Fe1-C <sub>C≡N</sub>	1.927(4)	1.891(4)	1.883(3)
Fe1-N <sub>Tp</sub>	1.993(3)	2.001(3)	2.003(2)
Fe2-N <sub>C≡N</sub>	2.121(3)	2.023(3)	1.994(2)
Fe2-N <sub>bnbpen</sub>	2.241(3)	2.200(3)	2.183(2)
π-π distances	3.400(2)-3.444(2)	3.360(2)-3.399(3)	3.338(3)-3.377(4)

**Table S3.** Selected bond angles ( $^{\circ}$ ) of 1·8CH<sub>3</sub>OH at different temperatures.

	1·8CH <sub>3</sub> OH 298 K	1·8CH <sub>3</sub> OH 165 K	1·8CH <sub>3</sub> OH 100 K
C1A–Fe1–C3	89.42(14)	91.91(13)	91.97(10)
C1A–Fe1–N4	177.46(13)	176.41(12)	176.29(9)
C1A–Fe1–N5	92.48(13)	91.65(12)	91.40(9)
C1A–Fe1–N6	89.58(13)	89.18(12)	89.34(9)
C2–Fe1–C1A	88.32(13)	90.25(13)	90.79(10)
C2–Fe1–C3	87.05(14)	88.31(13)	88.55(10)
C2–Fe1–N4	90.80(12)	90.76(12)	90.64(9)
C2–Fe1–N5	176.75(14)	176.72(12)	176.57(9)
C2–Fe1–N6	94.35(14)	94.20(13)	94.15(9)
C3–Fe1–N4	92.92(13)	91.57(12)	91.49(9)
C3–Fe1–N5	89.80(14)	88.95(13)	88.74(9)
C3–Fe1–N6	178.25(14)	177.26(13)	176.99(9)
N10–Fe2–N7	95.06(10)	93.33(10)	93.12(7)
N10–Fe2–N8	76.06(10)	76.46(10)	76.81(7)
N1–Fe2–N10	94.75(11)	95.94(11)	95.90(8)
N1–Fe2–N2	95.02(11)	96.86(11)	97.53(8)
N1–Fe2–N7	165.24(10)	165.28(11)	165.47(8)
N1–Fe2–N8	91.52(11)	90.41(10)	90.09(8)
N1–Fe2–N9	94.14(11)	93.71(11)	93.87(8)
N2–Fe2–N10	91.11(11)	91.22(10)	91.39(8)
N2–Fe2–N7	95.79(11)	94.35(10)	93.60(7)
N2–Fe2–N8	166.06(11)	166.32(10)	166.59(8)
N2–Fe2–N9	92.24(11)	93.03(11)	92.93(8)
N4–Fe1–N5	88.53(11)	87.50(11)	87.33(8)
N6–Fe1–N4	88.11(12)	87.32(11)	87.15(8)
N6–Fe1–N5	88.80(13)	88.49(12)	88.52(9)
N7–Fe2–N8	80.20(11)	80.64(10)	80.89(7)
N9–Fe2–N10	170.19(10)	168.92(10)	168.70(7)
N9–Fe2–N7	75.43(10)	76.16(10)	76.20(7)
N9–Fe2–N8	99.57(10)	98.06(10)	97.56(7)

Symmetry code: A = -x+1, -y+1, -z.

**Table S4.** Crystal data and structure refinement for **1**.

1			
CCDC	2220543	2220544	2183792
T /K	298	200	100
Formula	$C_{96}H_{88}B_2Fe_4N_{26}Cl_2O_8$		
Formula weight	2049.8		
Crystal system	Triclinic		
Space group	$P\bar{1}$		
<i>a</i> /Å	11.646(2)	11.684(2)	10.998(3)
<i>b</i> /Å	14.444(3)	14.378(3)	15.766(5)
<i>c</i> /Å	16.283(3)	16.243(3)	16.541(5)
$\alpha$ /°	107.241(8)	107.075(9)	110.445(4)
$\beta$ /°	94.910(8)	94.534(10)	93.745(5)
$\gamma$ /°	104.543(8)	104.418(9)	108.936(4)
<i>V</i> / Å <sup>3</sup>	2494.0(8)	2492.0(9)	2489.8(12)
<i>d<sub>calc</sub></i> (mg/m <sup>3</sup> )	1.365	1.366	1.367
$\mu$ / mm <sup>-1</sup>	3.85	3.86	3.92
<i>F</i> (000)	1058	1058	1058
Collected reflections	37304	29759	16395
Unique reflections	8204	8127	8090
<i>R</i> <sub>int</sub>	0.095	0.095	0.047
Goodness-of-fit on <i>F</i> <sup>2</sup>	1.02	1.04	1.03
<i>R</i> <sub>1</sub> [ <i>I</i> > 2σ ( <i>I</i> )]	0.072	0.079	0.089
<i>wR</i> <sub>2</sub> [ <i>I</i> > 2σ ( <i>I</i> )]	0.229	0.229	0.273

$$R_1 = \sum (|F_o| - |F_c|) / \sum |F_o|; wR_2 = [\sum w (|F_o| - |F_c|)^2 / \sum w F_o^2]^{1/2}.$$

**Table S5.** Selected bond lengths ( $\text{\AA}$ ) of **1** at different temperatures.

	<b>1<sup>298K</sup></b>	<b>1<sup>200K</sup></b>	<b>1<sup>100K</sup></b>
Fe1-C1	1.906(6)	1.920(5)	1.877(7)
Fe1-C2	1.913(6)	1.924(6)	1.862(7)
Fe1-C3	1.921(6)	1.926(6)	1.921(10)
Fe1-N4	1.976(4)	1.992(4)	1.989(5)
Fe1-N5	1.983(4)	1.986(4)	1.984(6)
Fe1-N6	1.956(5)	1.974(5)	1.970(7)
Fe2-N1	2.121(5)	2.104(4)	1.972(6)
Fe2-N2	2.102(5)	2.105(5)	1.983(6)
Fe2-N7	2.265(4)	2.268(4)	2.169(6)
Fe2-N8	2.259(4)	2.256(4)	2.185(6)
Fe2-N9	2.198(5)	2.194(5)	2.090(6)
Fe2-N10	2.203(5)	2.208(5)	2.101(6)
Fe1-C <sub>C≡N</sub>	1.913(6)	1.923(5)	1.887(8)
Fe1-N <sub>Tp</sub>	1.972(4)	1.984(4)	1.981(6)
Fe2-N <sub>C≡N</sub>	2.112(5)	2.105(4)	1.978(6)
Fe2-N <sub>bnbpen</sub>	2.231(5)	2.232(5)	2.136(6)
$\pi\text{-}\pi$ distances [ $\text{\AA}$ ]	3.322(4)-3.390(4)	3.180(5)-3.396(6)	3.155(4)-3.391(4)

**Table S6.** Selected bond angles ( $^{\circ}$ ) of **1** at different temperatures.

	1298 K	1200 K	1100 K
C1–Fe1–C3	88.0(2)	87.7(2)	90.4(3)
C1–Fe1–N4	178.89(2)	179.3(2)	177.7(3)
C1–Fe1–N5	94.0(2)	93.90(2)	92.3(3)
C1–Fe1–N6	91.4(2)	91.4(2)	90.2(3)
C2–Fe1–C1	87.0(2)	87.3(2)	90.3(3)
C2–Fe1–C3	88.8(2)	89.1(2)	87.8(3)
C2–Fe1–N4	91.88(2)	92.03(2)	90.9(2)
C2–Fe1–N5	178.66(2)	178.78(2)	176.8(3)
C2–Fe1–N6	91.3(2)	91.2(3)	92.9(3)
C3–Fe1–N4	91.9(2)	92.36(2)	91.5(3)
C3–Fe1–N5	90.4(2)	90.7(2)	90.2(3)
C3–Fe1–N6	179.4(2)	179.13(3)	179.1(3)
N4–Fe1–N5	87.12(2)	86.79(2)	86.6(2)
N6–Fe1–N4	88.62(3)	88.47(2)	87.8(2)
N6–Fe1–N5	89.59(2)	89.12(3)	89.1(3)
N10–Fe2–N7	98.81(2)	98.86(2)	95.7(2)
N10–Fe2–N8	76.26(2)	76.00(2)	77.2(2)
N1–Fe2–N10	90.93(3)	90.33(2)	92.3(3)
N1–Fe2–N2A	99.16(2)	98.91(2)	95.7(2)
N1–Fe2–N7	165.38(2)	165.91(2)	167.4(2)
N1–Fe2–N8	91.31(2)	91.36(3)	90.2(3)
N1–Fe2–N9	93.80(3)	94.21(17)	94.0(3)
N2A–Fe2–N10	90.59(3)	90.74(2)	90.8(2)
N2A–Fe2–N7	91.66(2)	91.66(3)	94.0(2)
N2A–Fe2–N8	163.37(3)	163.31(2)	166.9(2)
N2A–Fe2–N9	94.09(3)	94.58(2)	92.5(2)
N7–Fe2–N8	80.55(2)	80.64(2)	82.1(3)
N9–Fe2–N10	172.73(2)	172.39(2)	172.6(2)
N9–Fe2–N7	75.52(2)	75.58(2)	77.4(2)
N9–Fe2–N8	98.10(2)	97.77(3)	98.8(2)

Symmetry code: A = -x+2, -y+1, -z+2.

**Table S7.** Structural parameters for **1**·8CH<sub>3</sub>OH and **1** at high and low temperature.

Compd.		$\Sigma_{\text{Fe}}(^{\circ})$	$\zeta_{\text{Fe}}$	$\Theta_{\text{Fe}}(^{\circ})$	
<b>1</b> ·8CH <sub>3</sub> OH 298 (100) K	Fe1	20.94 (20.81)	0.19 (0.36)	70.67 (60.71)	[FeC <sub>3</sub> N <sub>3</sub> ]
	Fe2	77.52 (72.11)	0.33 (0.51)	223.37 (203.21)	[FeN <sub>6</sub> ]
<b>1</b> 298 (100) K	Fe1	21.72 (17.46)	0.18 (0.28)	60.44 (53.81)	[FeC <sub>3</sub> N <sub>3</sub> ]
	Fe2	76.12 (67.12)	0.32 (0.43)	242.79 (202.39)	[FeN <sub>6</sub> ]

[a]  $\Sigma_{\text{Fe}}$ : the sum of |90-a| for the 12 cis-N-Fe-N angles around the iron atom; [b]  $\zeta_{\text{Fe}}$ : the average of the sum of the deviation of 6 unique metal-ligand bond lengths around the central metal atom(Fe)from the average value. [c]  $\Theta_{\text{Fe}}$ : the sum of the deviation of 24 unique torsional angles between the ligand atoms on opposite triangular faces of the octahedron viewed along the pseudo-threefold axis ( $\theta_i$ ) from 60°. All of these data are obtained through the OctaDist software.<sup>1</sup>

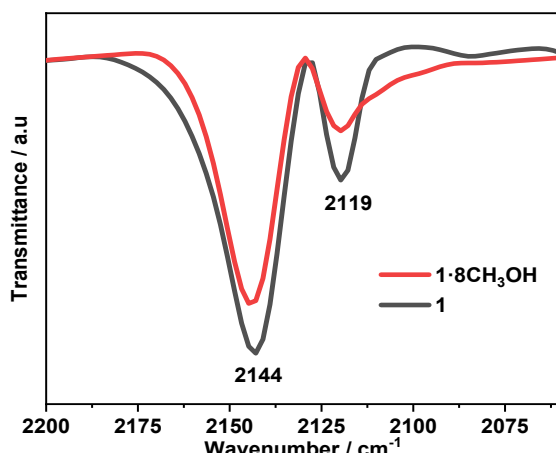


**Figure S7.** IR spectra for **1**·8CH<sub>3</sub>OH and **1** at room temperature.

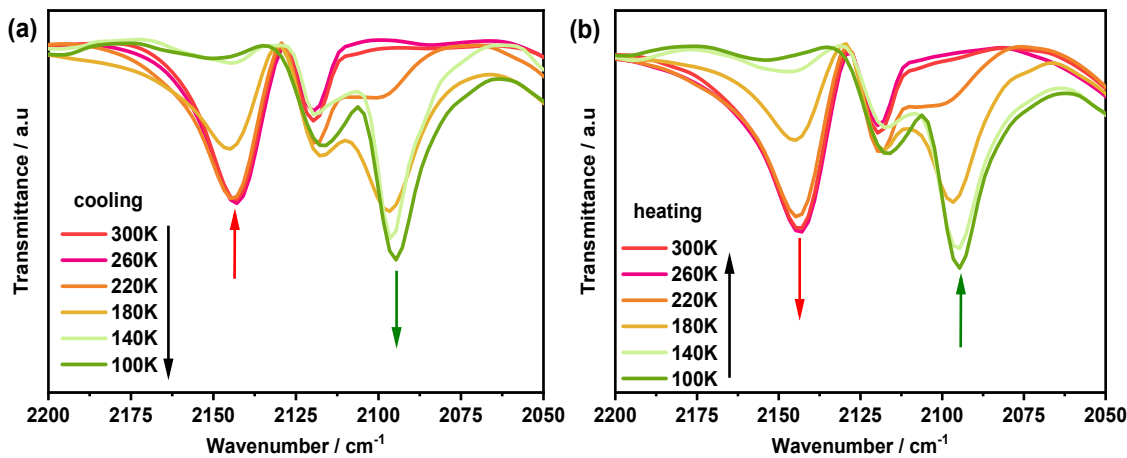


**Figure S8.** Variable temperature solid state FT-IR spectra for **1**·8CH<sub>3</sub>OH: (a) in cooling (300 → 100 K) and (b) heating modes (100 → 300 K)

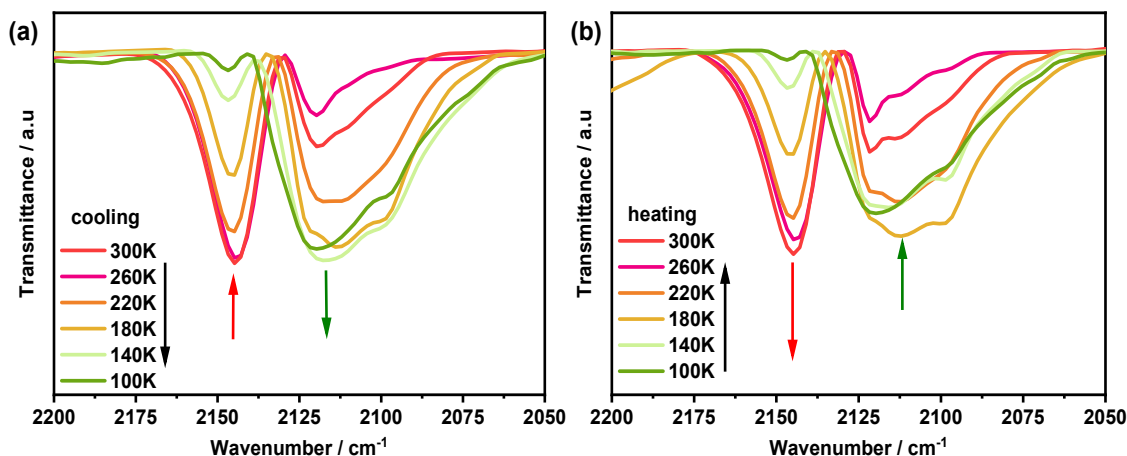


**Figure S9.** Variable temperature solid state FT-IR spectra for **1**: (a) in cooling (300 → 100 K) and (b) heating modes (100 → 300 K).

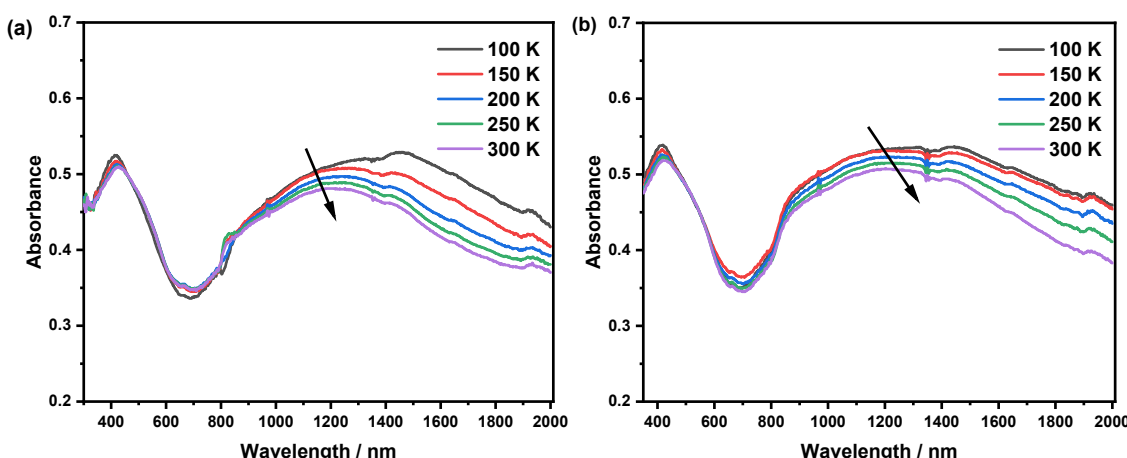


**Figure S10.** Variable-temperature solid-state UV-vis spectra for **1**·8CH<sub>3</sub>OH (a) and **1** (b) in heating mode.

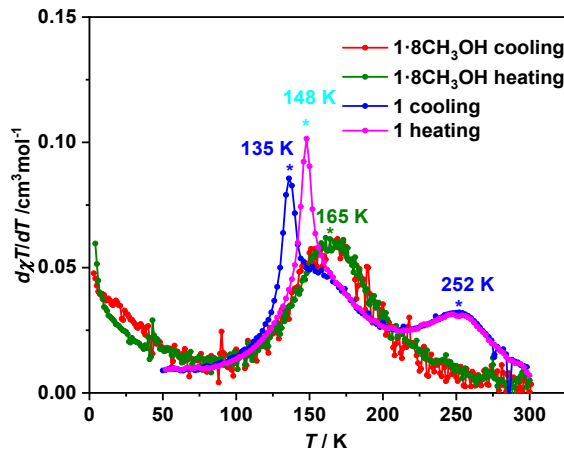


**Figure S11.** Plots of  $d\chi_T/dT$  vs. temperature for  $1\cdot8\text{CH}_3\text{OH}$  and **1**.

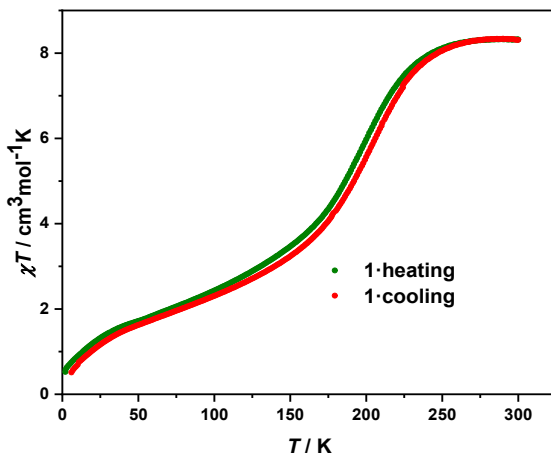


**Figure S12.** Plots of  $\chi_M T$  vs. temperature for  $1\cdot8\text{CH}_3\text{OH}$  and **1** ( $3 \text{ K}\cdot\text{min}^{-1}$  from 2 to 300 K)

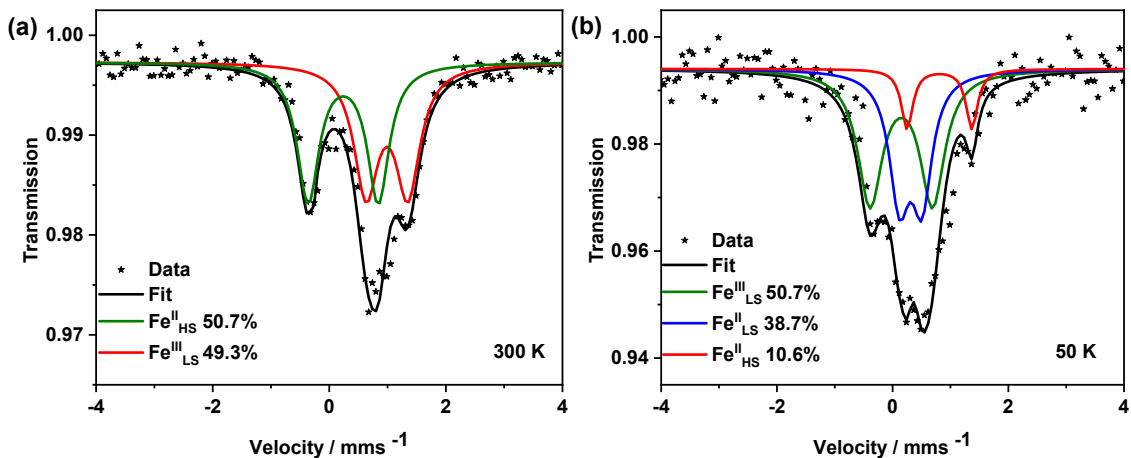


**Figure S13.**  $^{57}\text{Fe}$  Mössbauer spectra of  $1\cdot8\text{CH}_3\text{OH}$  at 300 K (a) and 50 K (b).

**Table S8.** Mössbauer spectrum data of **1**·8CH<sub>3</sub>OH and **1**.

	<b>T</b> (K)	<b>Fe site</b>	<b>δ</b> (mm s <sup>-1</sup> )	<b>ΔE<sub>Q</sub></b> (mm s <sup>-1</sup> )	<b>Aera (%)</b>
<b>1</b> ·8CH <sub>3</sub> OH	300	Fe <sup>II</sup> <sub>HS</sub>	0.99	0.72	50.7
		Fe <sup>III</sup> <sub>LS</sub>	0.24	1.20	49.3
	50	Fe <sup>II</sup> <sub>HS</sub>	0.81	1.12	10.6
		Fe <sup>II</sup> <sub>LS</sub>	0.31	0.39	38.7
	300	Fe <sup>III</sup> <sub>LS</sub>	0.15	1.08	50.7
		Fe <sup>II</sup> <sub>HS</sub>	1.10	0.89	49.4
<b>1</b>	200	Fe <sup>III</sup> <sub>LS</sub>	0.19	1.24	50.6
		Fe <sup>II</sup> <sub>HS</sub>	0.91	1.34	24.7
	30	Fe <sup>II</sup> <sub>LS</sub>	0.31	0.30	25.4
		Fe <sup>III</sup> <sub>LS</sub>	0.12	0.90	50.0
	30	Fe <sup>II</sup> <sub>LS</sub>	0.46	0.45	50.8
		Fe <sup>III</sup> <sub>LS</sub>	0.01	1.02	49.2

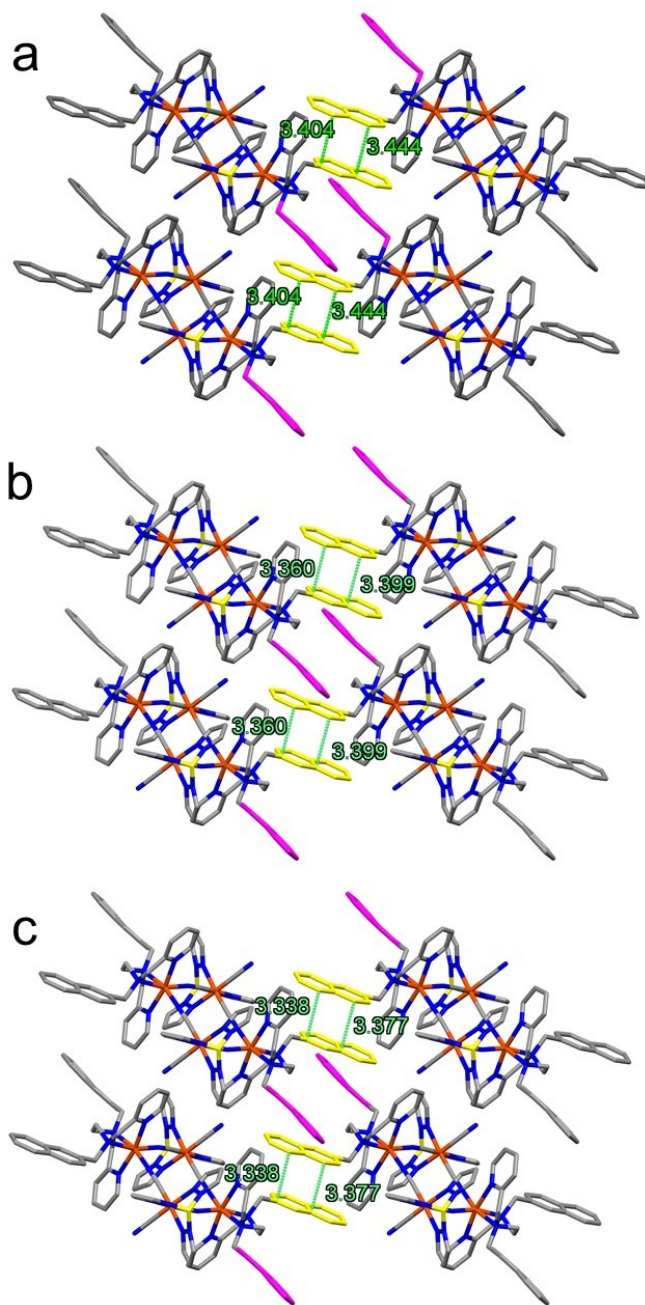


**Figure S14.** Packing diagrams of **1·8CH<sub>3</sub>OH** (a: 298 K, b: 165 K, c: 100 K) illustrating intermolecular π-π interactions between adjacent bnbpn ligands along the b-axis. All hydrogen atoms are omitted for clarity.

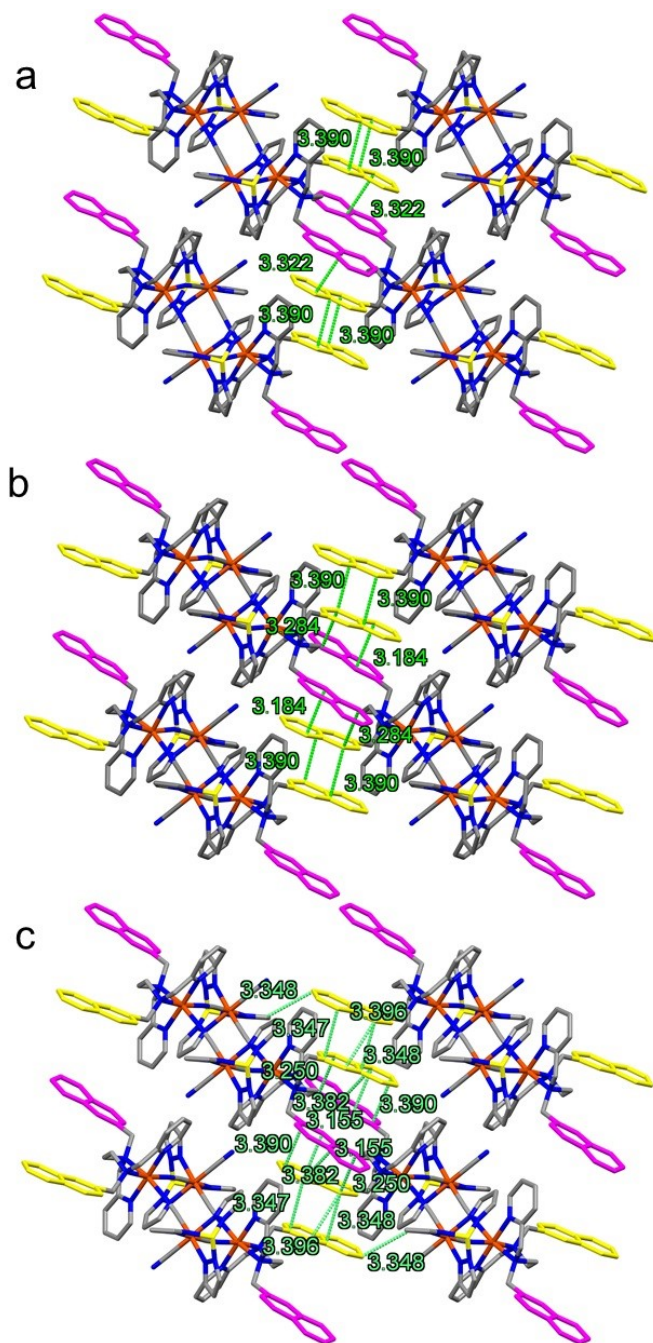


**Figure S15.** Packing diagrams of **1** (a: 298 K, c: 200 K, e: 100 K) illustrating intermolecular  $\pi$ - $\pi$  interactions between adjacent bnbpn ligands along the b-axis. All hydrogen atoms are omitted for clarity.

The amount of solvent molecules within the crystal structure affects how they pack as well as intermolecular  $\pi$ - $\pi$  interactions between adjacent naphthyl groups of bnbpn, the intermolecular  $\pi$ - $\pi$  interactions continued to decrease during the cooling process from 298 K to 100 K.

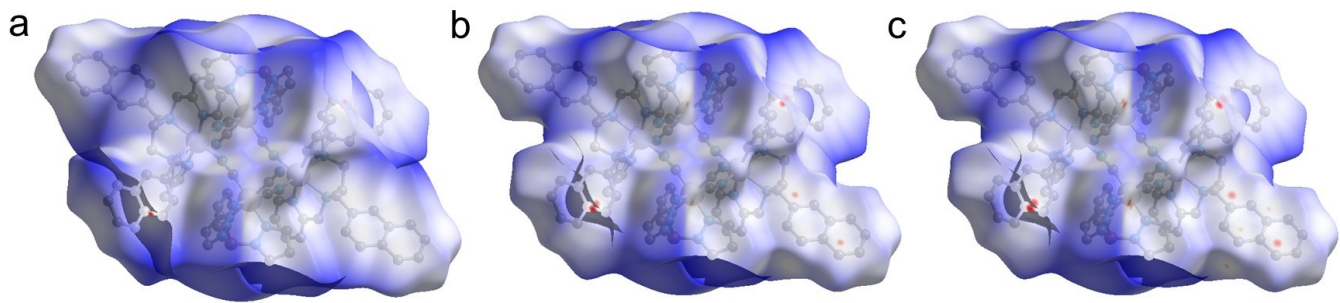


**Figure S16.** Hirshfeld surface of **1**·8CH<sub>3</sub>OH (a: 298 K, b: 165 K, c: 100 K) mapped with  $d_{norm}$  function.

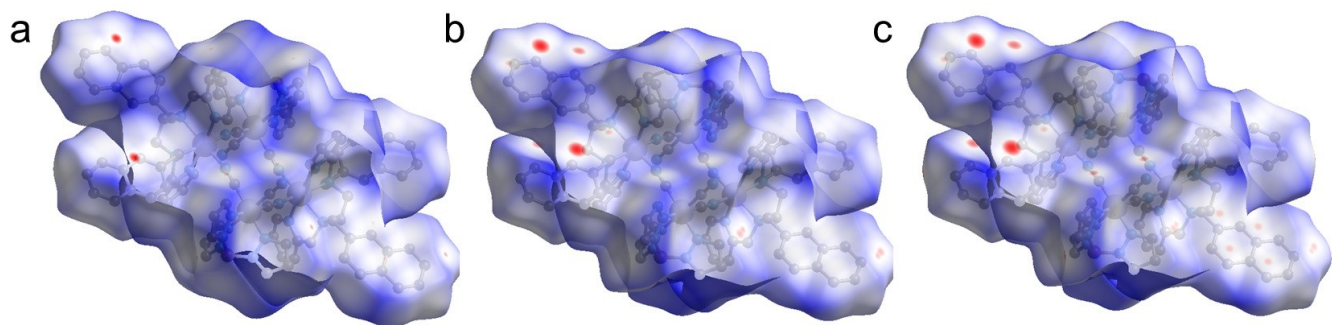


**Figure S17.** Hirshfeld surface of **1** (a: 298 K, b: 200 K, c: 100 K) mapped with  $d_{norm}$  function.

The Hirshfeld surface map also showed that the intermolecular interaction force is very weak at 298 K between the naphthalene rings, while the intermolecular interaction force near the naphthalene ring was strong at 100 K. It was clear that low temperature stabilized the LS state of the complex.

1. R. Ketkaew, Y. Tantirungrotechai, P. Harding, G. Chastanet, P. Guionneau, M. Marchivie and D. J. Harding, *Dalton Trans.*, 2021, **50**, 1086-1096.